International Journal of Waste Resources

Abdelrahman et al., Int J Waste Resour 2015, 5:3
DOI: 10.4172/2252-5211.1000180

Research Article Open Access

Effect of Used Motor Oil on the Macro and Micromechanical Properties of Crumb Rubber Modified Asphalt

Magdy Abdelrahman, Mohyeldin Ragab* and Daniel Bergerson

Department of Civil and Environmental Engineering North Dakota State University, USA

Abstract

The need to be more environmentally conscious has recently shifted toward the forefront of society. With this new focus on environmentally responsible behavior comes the practice of using recycled materials in construction when possible. Used motor oil (UMO) is an example of waste materials that can be utilized in numerous applications to alleviate its environmental disposal burden. In the current work, the effect of UMO on the internal structure of crumb rubber modified asphalt is investigated. This is carried out by employing rheological analysis including dynamic shear rheometer and microindentation testing. Rheological analysis was employed to determine the change in the phase angle (δ) as well as the complex modulus (G*) of the UMO modified asphalts as well as the crumb rubber modified asphalt (CRMA), in addition, temperature sweep viscoelastic analysis was employed to investigate the change in internal structure of the produced modified asphalts. Microindentation analysis was utilized to determine the hardness and elastic modulus of the modified asphalt liquid phase. Microindentation tests served to simulate the effect of UMO on the behavior of the thin asphalt layer over the aggregate which has a thickness measured in microns. Results indicate that the utilization of UMO only as a modifier to asphalt severely deteriorates the macro and micro mechanical properties of the binder. Combining CRM with UMO as modifiers to asphalt had better results. It is suggested to use UMO at a rate of 3%, or less, by asphalt weight.

Keywords: Used motor oil; Crumb rubber modifier; Three dimensional network structure; Crumb rubber modified asphalt

Abbreviations: CRM: Crumb Rubber Modifier; UMO: Used Motor Oil; CRMA: Crumb Rubber Modified Asphalt; 3D: Three Dimensional

Introduction

Each year, two hundred million gallons of used oil are improperly disposed of [1]. In recent years, attention has been brought to the need to preserve the environment and its resources for future generations. This can be achieved through the utilization of waste materials, in addition to limiting the use of virgin products. Used motor oil (UMO) and crumb rubber modifier (CRM) are both waste materials that can be implemented in the paving industry. Although both materials have been investigated separately, up to this point no research has been dedicated to investigating the combined effect of such binder modifiers on the binder's rheological, internal and micromechanical properties.

CRM is an example of a recycled material that is incorporated into asphalt pavement. CRM is made from recycled tires. Asphalt is made up of continuous three- dimensional associations of polar molecules that are dispersed in a fluid of nonpolar or relatively low-polarity molecules [2]. Associations of different strengths are created by the polar functions within asphalt [3]. The typical viscoelastic properties for neat asphalts are the result of continuous formation and breakage of these associations under the effect of external factors such as shear stresses and temperature variations [2].

Research by Dedene et al. [4] and by Villanueva et al. [5] suggests that UMO can be used as rejuvenator for existing and recycled asphalt pavement and can enhance low temperature service performance.

In previous work by this research group it was verified that the existence of 3D network structures occurs in CRMA [6]. The effect of the developed three dimensional (3D) network structure in the liquid phase of CRMA at the end of the interaction time has been shown to be essential and deterministic to the enhancement of both the G* and δ of CRMA [6]. However, the effect of addition of UMO to asphalt that is either neat or modified with CRM needs further investigation. The interaction of CRM and asphalt results in a non-homogeneous mixture due to the fairly consistent physical shape of CRM when treated with the binder. Thus it is essential to understand how the UMO would alter the behavior of the asphalt-CRM mix. In another work by us, we investigated the environmental impact of UMO during the modification with asphalt [7]. We proved through air testing and batch leaching that interaction temperature, interaction time, and binder grade affect the amount of Benzene, Toluene, Ethylbenzene, and Xylenes (BTEX) leached from modified asphalt binder. In addition, we found that the binders modified with both CRM and UMO released less BTEX to both leachate and the air at the end of interaction time, indicating that CRM retains BTEX and prevents it from being released into the environment when used in conjunction with UMO [7].

The aim of this work is to investigate the effect of addition of UMO to neat as well as CRMA and also investigate how it affects the modified asphalt rheological (stiffness and elasticity), internal structure and micromechanical properties. This is achieved by investigating the change in the internal network structure of the modified asphalt through monitoring the change in the physical properties of asphalt through single point and temperature sweep viscoelastic tests as well as microindentation analysis. In addition, the utilization of microindentation serves to simulate the behavior of a thin layer or coating of asphalt such as that laid on the surface of aggregate.

***Corresponding author:** Mohyeldin Ragab, Ph.D. Candidate, Department of Civil and Environmental Engineering, North Dakota State University, Tel: 701-318-4401; Fax: 701-231-6185; E-mail: Mohyeldin.ragab@ndsu.edu

Received June 27, 2015; **Accepted** July 21, 2015; **Published** July 25, 2015

Citation: Abdelrahman M, Ragab M, Bergerson D (2015) Effect of Used Motor Oil on the Macro and Micromechanical Properties of Crumb Rubber Modified Asphalt. Int J Waste Resour 5: 180. doi: 10.4172/2252-5211.1000180

Materials and Methods

Processing

Raw materials: In the current work, one asphalt binder was investigated in combination with one type of crumb rubber. The asphalt was a PG 64-22 based on the superpave grading system. The CRM was a cryogenic processed CRM from a mixed source of scrap tires. The CRM particle size was smaller than mesh #30 and larger than mesh #40, according to the US standard system.

Collected used motor oils have been tested for Benzene, Toluene, Ethyl-benzene, and Xylenes (BTEX) content and it was verified that the utilized UMO in the current experiments has less BTEX content than what is allowed by the United States Environmental Protection Agency (US-EPA) Maximum Contaminants Levels (MCLs) during leaching experiments and also from air tested samples above the interactions carried out in the lab.

Asphalt-CRM interactions: The interactions were conducted in 1 gallon cans, and a heating mantle connected to a bench type controller with a long temperature probe (12") was used to heat the material. A high shear mixer was used to mix the binder and crumb rubber. The amount of CRM was controlled to be either 10% or 20% of the initial asphalt binder weight in selected interactions. The UMO percentage varied from 3% to 9% of the final binder weight. Interactions were conducted for 120 minutes under one of two different temperatures (160 and 190°C) and a single mixing speed (30 Hz) for each temperature utilized. Samples were taken at 2, 30, and 120 minutes of interaction time and kept at -12°C to avoid any unwanted reactions. All interactions in this research were carried out under controlled atmosphere of nitrogen gas to prevent any oxidation. A specific coding for the samples was adopted in the current work, starting with the asphalt type, HU-64, followed by the interaction temperature, interaction speed, UMO percentage, and lastly CRM percentage. Table 1 illustrates the list of interactions utilized in this research work.

Characterization

Extraction of liquid phase: The liquid phase of CRMA was extracted by removing the non-dissolved CRM particles from the CRMA matrix. In this regard, the required amount of CRMA sample was heated to 165˚C and drained through mesh #200 (75 µm) in the oven at 165˚C for 25 minutes. The extracted liquid phase was stored at -12˚C immediately to prevent any unwanted reactions.

Dynamic mechanical analysis: Dynamic Shear Rheometer from Bohlin Instruments CVO, (Worcestershire, UK) was used for viscoelastic analysis of neat modified asphalt samples and their liquid phase. Single point test and temperature sweep test were performed on the samples.

The single point test was performed on all modified asphalt samples before separation of the liquid phase at 64°C and 10 radian/sec using 25 mm diameter parallel plates. The temperature sweep test was performed on the liquid phase of modified asphalt at a temperature range of 10°C to 70°C with 6°C increments. 25 mm diameter plates were used for tests that conducted above 45°C, and 8 mm diameter plates were used for tests that were conducted below 45°C.

The gap between plates for CRMA samples was selected to be 2 mm, which is the minimum gap size that does not affect the results due the presence of CRM particle. For samples without CRM and for the liquid phase, the gap was selected to be 1 mm. For all tests that were conducted at temperatures below 45°C using the 8 mm diameter plates, the 2 mm gap size was selected, regardless of the type of the sample.

Preparation of CRMA microindentation samples: The procedure of asphalt sample preparation for indentation testing was adapted from literature [8,9]. The preparation of the CRMA liquid phase thin film involved the utilization of a glass slide surface that was covered with a high temperature resistant tape. A rectangular window of size 1.5x0.5″ (38.1x12.7 mm) was made inside the high temperature resistant tape. Following that, CRMA was heated to 160°C and poured into the square window in the high temperature resistant tape. In order to have a smooth CRMA surface, the glass substrate coated with CRMA was placed in the oven at 160°C for 5 min. After that, the glass substrate was cooled down to room temperature. The CRMA film thickness ranges were controlled to be between 550–600 µm to insure that the measured values for hardness and elastic modulus are not affected by the glass substrate.

Microindentation tests procedure: In this research work, a FISCHERSCOPE HM2000S indenter was utilized for the indentation tests. Indentation tests were carried out using a tungsten carbide metal spherical tip of diameter 2mm that conforms with ISO 14577-3. All indentation tests were carried out under load control mode. The indentation load configuration was programmed to start with a constant loading rate followed by a holding period at maximum load and finishing with an unloading rate similar to the loading one. The maximum load was 5 mN. The loading and unloading times were 20 seconds. The dwell time at maximum load was 60 seconds to minimize the viscous effect on the unloading portion of the material [8-10]. All tests were carried out at ambient temperature. For each sample a minimum of 5 indentations were carried out to determine the hardness and elastic modulus. A minimum distance of 6 mm between two

#'	Code	Interaction temperature (°C)	Mixing speed (Hz)	UMO percentage	CRM percentage
1	HU-64-160-30-3% UMO	160	30	3	0
2	HU-64-160-30-3% UMO-10% CRM	160	30	3	10
3	HU-64-160-30-10% CRM	160	30	0	10
4	HU-64-160-30-9% UMO	160	30	9	0
5	HU-64-160-30-9% UMO-20% CRM	160	30	9	20
6	HU-64-160-30-20% CRM	160	30	0	20
7	HU-64-190-30-3% UMO	190	30	3	0
8	HU-64-190-30-3% UMO-10% CRM	190	30	3	10
9	HU-64-190-30-10% CRM	190	30	0	10
10	HU-64-190-30-9% UMO	190	30	9	0
11	HU-64-190-30-9% UMO-20% CRM	190	30	9	20
12	HU-64-190-30-20% CRM	190	30	0	20

Table 1: List of interactions.

indentations was utilized to avoid the pile up and sink-in effect for successive indentations and also to conform to the ASTM guidelines that require a distance of at least 6 indent radii from the previous indentation point. In this work the Oliver and Pharr method was utilized for the analysis of the indentation test data [11]. The Oliver and Pharr method not only accounts for the curvature in the unloading data but also provides a physically justifiable approach for determining the indentation depth to be used in conjunction with the indenter shape function to establish the contact area at peak load [11]. The analysis starts by defining a reduced modulus E_r that accounts for the effects of a non-rigid indenter on the load-indentation behavior as follows [12]:

$$\frac{1}{E_r} = \frac{1-\upsilon_s^2}{E_s} - \frac{1-\upsilon_i^2}{E_i} \quad \text{..(Eq.1)}$$

where E_s=Young's modulus of the sample; υ_s=Poisson's ratio of the sample; E_i=Young's modulus of indenter, υ_i=Poisson's ratio of indenter; and E_r=reduced modulus.

The unloading portion of the indentation curve relates to the reduced modulus as follows [11,13]:

$$E_r = \frac{\sqrt{\pi}}{2}\frac{S}{\sqrt{A}} \quad \text{(Eq.2)}$$

where S=dP/dh=initial unloading stiffness and A=contact area.

To determine the initial unloading stiffness, Oliver and Pharr utilized curve fitting of the indentation depth versus loading/unloading data using the following power law function [11]:

$$P = \alpha(h - h_f)^2 \quad \text{....(Eq.3)}$$

where h=any depth of penetration; h_f =unrecoverable or plastic depth; and α and m=constants.

In this regard, m is a power-law exponent that is related to the geometry of the indenter [8]. The initial unloading slope S is determined by differentiating Eq. 3 and evaluating the derivative at the peak load and displacement [8].

Based on Oliver and Pharr's approach, the total displacement h is given as [11]:

$$h = h_c + h_s \quad \text{.....(Eq.4)}$$

where h_c is the vertical distance along which contact is made (contact depth) and h_s is the displacement of the surface at the perimeter of the contact [11]. The contact depth h_c can be determined from the experimental data by extrapolating the tangent line to the unloading curve at the maximum loading point down to zero loads [8,11]. h_s can be estimated from the intercept value for depth hi that relates to the contact depth h_c associated with the maximum loading point as follows [11]:

$$h_s = h_{max} - \varepsilon\frac{P_{max}}{S} \quad \text{.....(Eq.5)}$$

where Ɛ=geometric constant and P_{max} is the maximum indentation load.

The hardness can be obtained as follows [11]:

$$H = \frac{P_{max}}{A} \quad \text{(Eq.6)}$$

where **A**=projected area of contact at the peak load.

Results and Discussion

Figure 1 illustrates the rheological properties; (a) Complex modulus (G*) and (b) phase angle (δ) for the samples interacted at 160°C with 3% UMo, 10% CRM or both modifiers.

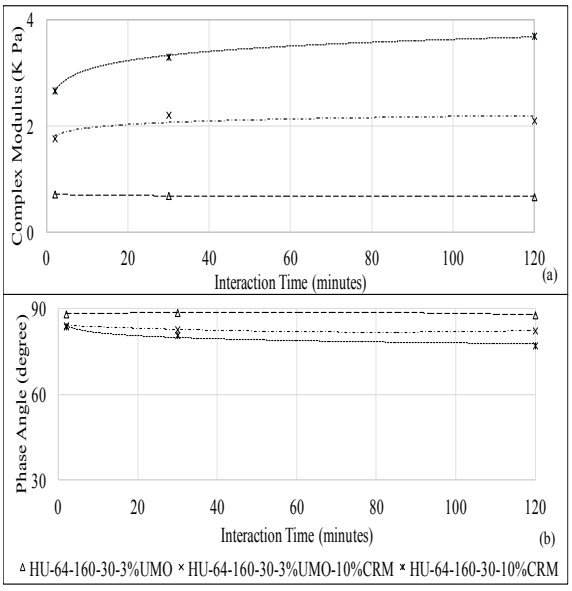

Figure 1: Rheological properties of the samples interacted with 3% UMO, 10% CRM, or both at 160C and 30Hz: (a) G* and (b) δ.

As shown in the Figure, the addition of 3% UMO to the asphalt resulted in deterioration in both the G* and δ. On the other hand, upon the utilization of 10% CRM only, enhancement in both the G* and δ was observed.

The combined use of 10% CRM and 3% UMO had a plateau effect for both the G* and δ values, but with values tending to slightly deteriorate at the end of interaction time (120 minutes). At such interaction temperature (160°C) and with the utilization of medium interaction speed (30Hz), the prevalent behavior observed in the swelling of the CRM particles with the low molecular weight fractions from asphalt and/or oil leading to minor enhancement of both the G* and δ [14]. On the other hand, the addition of UMO only to asphalt resulted in the disturbance of the asphalt's continuous three-dimensional associations leading to the observed deterioration in both G* and δ for the sample modified with 3% UMO only.

Figures 2a and 2b illustrates the rheological properties (G*) and (δ) for the samples interacted at 160°C with 9% UMO, 20% CRM, or both modifiers, respectively. A marked difference can be seen in the enhancement of both rheological parameters (G* and δ) for the sample with 20% CRM; this is due to the swelling of CRM and decrease of enter-particle distance [15]. In addition, for the sample with 20% CRM and 9% UMO, deterioration can be observed after 30 minutes of interaction time in both rheological parameters and continues until the end of the interaction time (120 minutes). This can result from the increased amount of UMO (9%) that significantly disturbed the asphalt's continuous three-dimensional associations, even in the presence of 20% CRM. This behavior of severe deterioration in both G* and δ was largely manifested in the sample with 9% UMO only.

Figure 3 illustrates the rheological properties; (a) Complex modulus (G*) and (b) phase angle (δ) for the samples interacted at 190°C with 3% UMO, 10% CRM, or both modifiers.

A distinctive behavior can be seen for the samples with 10% CRM and 3% UMO. There is continuous enhancement in both the G* and δ alongside the interaction time. Similar enhancements, with higher extent, can be seen for the sample with 10% CRM only. At such combination of moderate interaction temperature (190°C) and mixing speed (30 Hz) the interaction of CRMA involves not only the swelling of the CRM but also the occurrence of devulcanization processes of CRM that lead to the release of CRM components into the liquid phase of asphalt. This results in enhancements in the network structure of the CRMA whether UMO is present or not. On the other hand, the use of 3% UMO only resulted in deterioration in both the G* and δ as a result of the disturbance of the network structure of asphalt, as explained earlier.

Figures 4a and 4b illustrates the rheological properties (G*) and (δ) for the samples interacted at 190°C with 9% UMO, 20% CRM, or both modifiers, respectively.

As shown previously for the sample interacted at 160°C, a marked difference can be seen in the enhancement of both rheological parameters (G* and δ) for the sample with 20% CRM; this is due to the swelling of CRM as well as the occurrence of devulcanization at such interaction temperature (190°C) [16]. In addition, for the sample with 20% CRM and 9% UMO, unlike the behavior for the samples at 160°C, enhancements can be observed after 30minutes of interaction time in both rheological parameters and continue through the end of the interaction time (120 minutes). On the other hand, severe deterioration in both G* and δ was largely manifested in the sample with 9% UMO only.

Figure 5 illustrates the temperature sweep viscoelastic properties of the liquid phase for rheological properties (G*) and (δ) for the samples interacted at 160°C with 3% UMO, 10% CRM, or both modifiers after 120 minutes of interaction time, respectively.

In Figure 5, results show agreement with other studies which have shown that the CRM modification of asphalt mainly affects its high temperature properties and by decreasing the testing temperature the changes in physical properties reduce to a marginal level [5]. Results in Figure 5b show that the behavior of the δ lacks the presence of a plateau behavior, indicating lack of network structure in the liquid phase of modified asphalts [17,18].

Figure 6 shows the temperature sweep viscoelastic properties of liquid phase for rheological properties (G*) and (δ) for the samples interacted at 160°C with 9% UMO, 20% CRM, or both modifiers after 120 minutes of interaction time, respectively. It can be seen from the Figure that the behavior of the samples with UMO is almost similar with or without CRM addition. This indicates that the addition of the UMO significantly annihilated the network associations within the modified asphalt liquid phase.

Figure 7 shows the temperature sweep viscoelastic properties of the liquid phase for rheological properties (G*) and (δ) for the samples interacted at 190°C with 3% UMO, 10% CRM, or both modifiers after 120 minutes of interaction time, respectively. Results in Figure 7b show a distinctive behavior. Where, similarity can be observed between the behavior of both samples with 10% CRM only or 10% CRM and 3% UMO before 20°C and after 50°C. This indicates that the released components of the CRM in asphalt, in the presence of UMO, at certain interaction temperature (190°C and 30Hz) are capable of forming internal network in the asphalt matrix. The effect of such network was previously manifested by the enhancement in both G* and δ values of such sample as compared to the sample with 10% CRM only (illustrated in Figures 3a and 3b).

Figure 8 shows the temperature sweep viscoelastic properties of liquid phase for rheological properties (G*) and (δ) for the samples interacted at 190°C with 9% UMO, 20% CRM, or both modifiers after 120 minutes of interaction time, respectively.

Figure 8a, indicates that the G* values of the samples having UMO, either with or without CRM, are of similar values, in contrast with the samples with CRM only. As can be seen from Figure 8b, the behavior of the samples with 20% CRM and 9% UMO shows an intermediate trend between those that have 20% CRM only and those that contain 9% UMO only.

Figure 9 illustrates (a) the force vs. indentation depth profiles and (b) comparison of hardness and elastic modulus for the samples interacted at 160°C with 3% UMO, 10% CRM, or both modifiers, after 120 minutes of interaction time.

As can be seen from Figure 9a, the max load values show a continuous decrease during the dwell time, similar observations were recorded in the literature for the indentation of asphalt [8]. This was explained in terms of the decrease in contact area due to delayed (viscous) flow of asphalt binders at the indentation location [8]. Another reason is the minute scale load carrying capacity of the asphalt binders and binder softening which results in it being virtually impossible to keep the maximum applied load constant [8]. For the sample with only 3% UMO, the indentation depth was about 45 μm. For the sample with 10% CRM and 3% UMO the indentation depth was about 38 μm. However, upon utilizing 10% CRM only, further reduction in the indentation

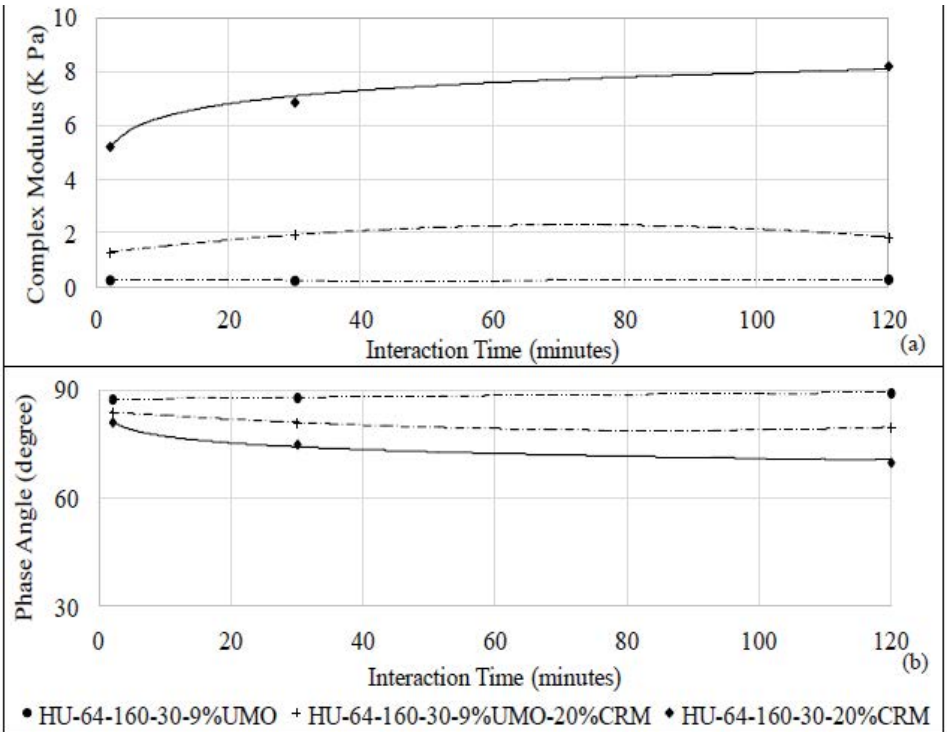

Figure 2: Rheological properties of the samples interacted with 9% UMO, 20% CRM or both at 160°C and 30Hz: (a) G* and (b) δ.

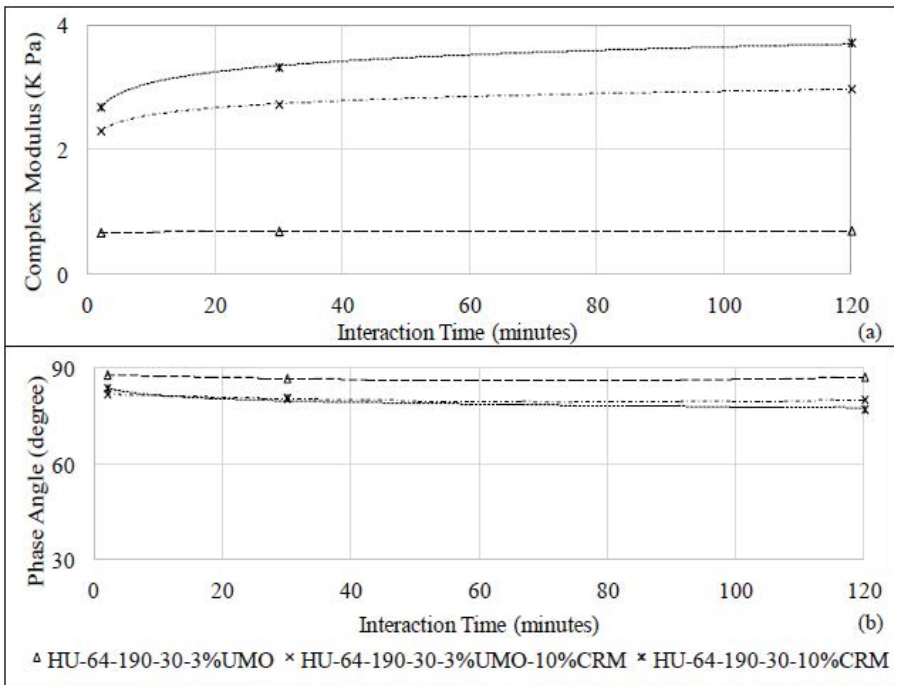

Figure 3: Rheological properties of the samples interacted with 3% UMO, 10% CRM or both at 190°C and 30Hz: (a) G* and (b) δ.

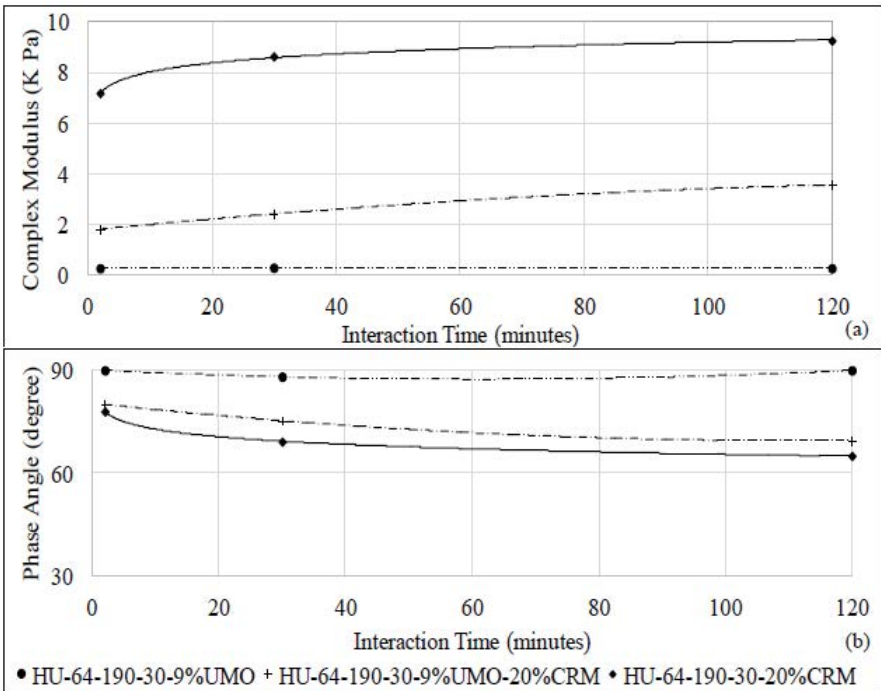

Figure 4: Rheological properties of the samples interacted with 9% UMO, 20%CRM or both at 190°C and 30Hz: (a) G* and (b) δ.

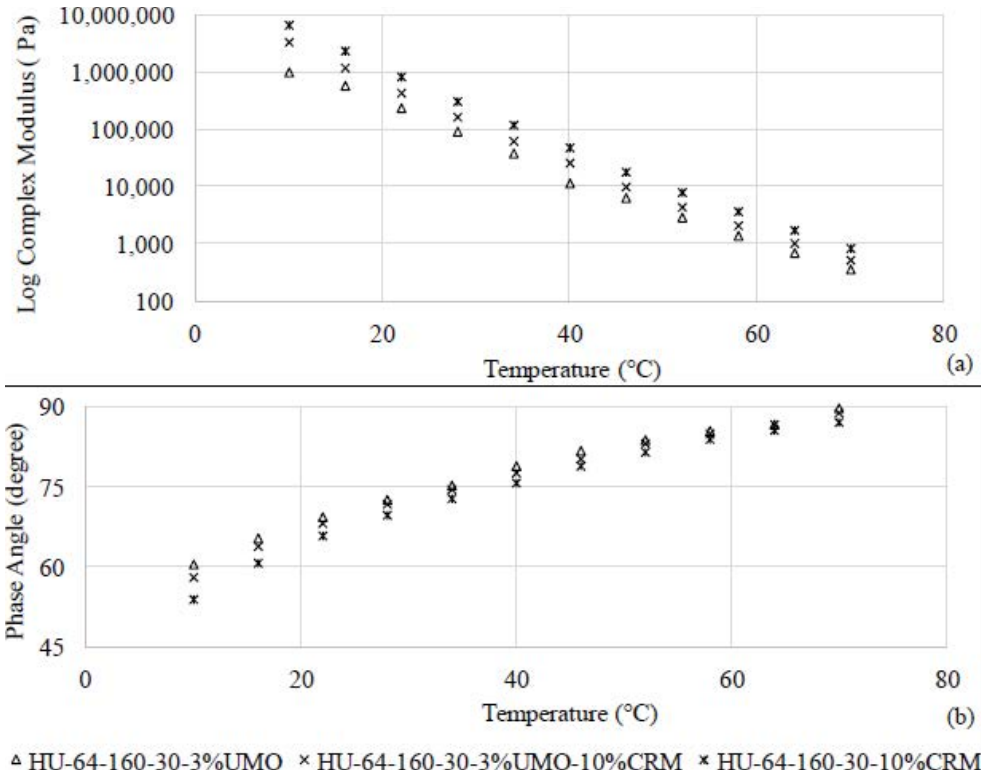

Figure 5: Temperature Sweep Viscoelastic Properties of Liquid Phase samples interacted with 3% UMO, 10% CRM or both at 160°C and 30Hz: (a) G* and (b) δ.

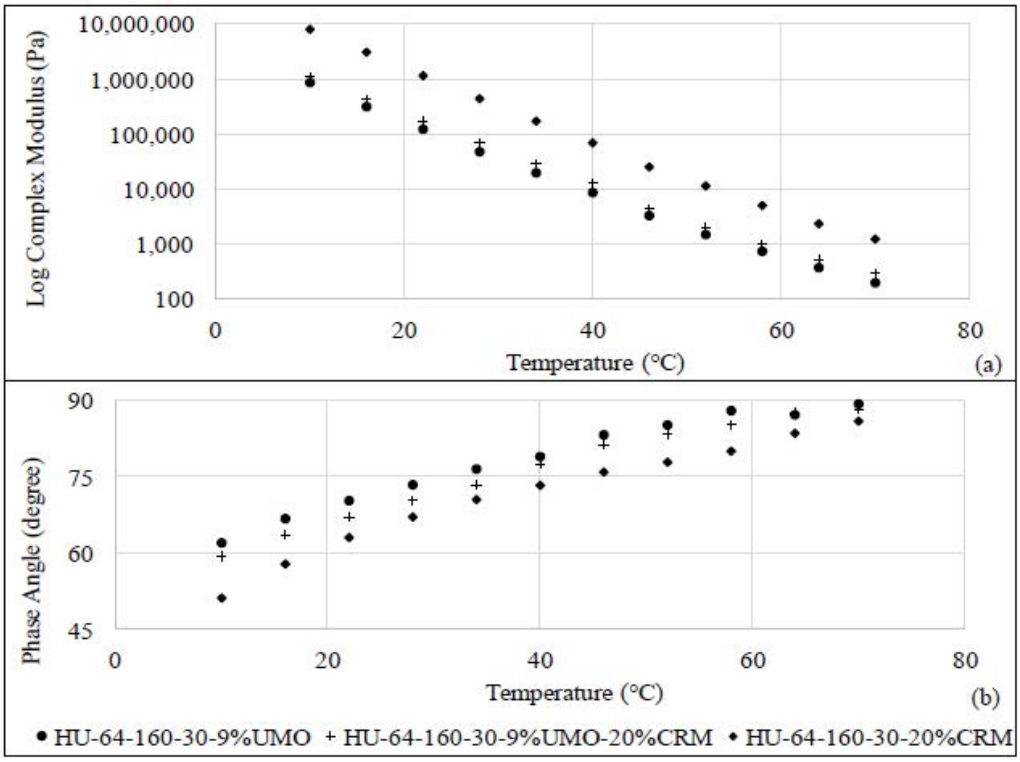

Figure 6: Temperature Sweep Viscoelastic Properties of Liquid Phase samples interacted with 9% UMO, 20% CRM or both at 160°C and 30Hz: (a) G* and (b) δ.

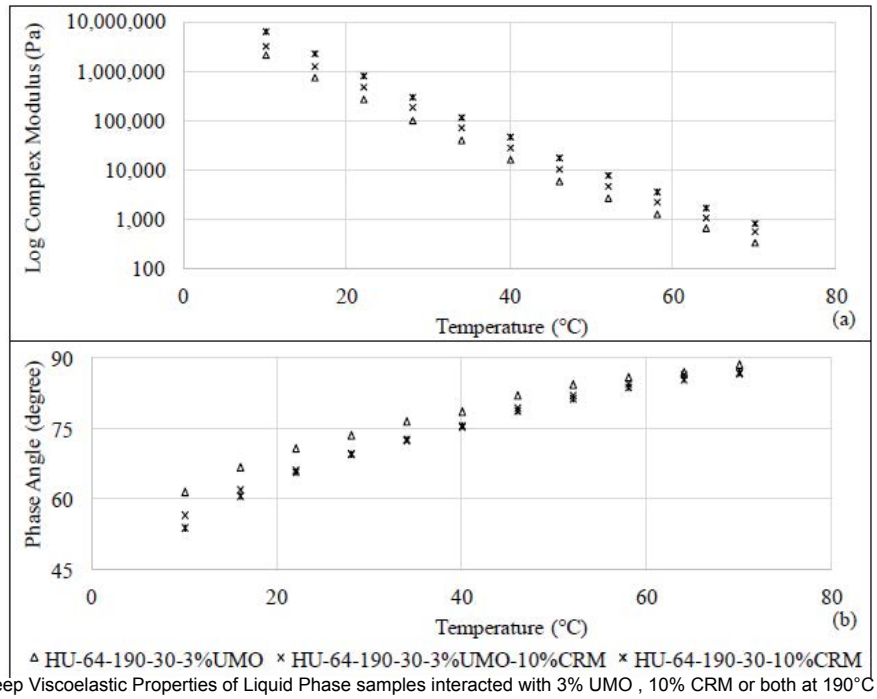

Figure 7: Temperature Sweep Viscoelastic Properties of Liquid Phase samples interacted with 3% UMO , 10% CRM or both at 190°C and 30Hz: (a) G* and (b) δ.

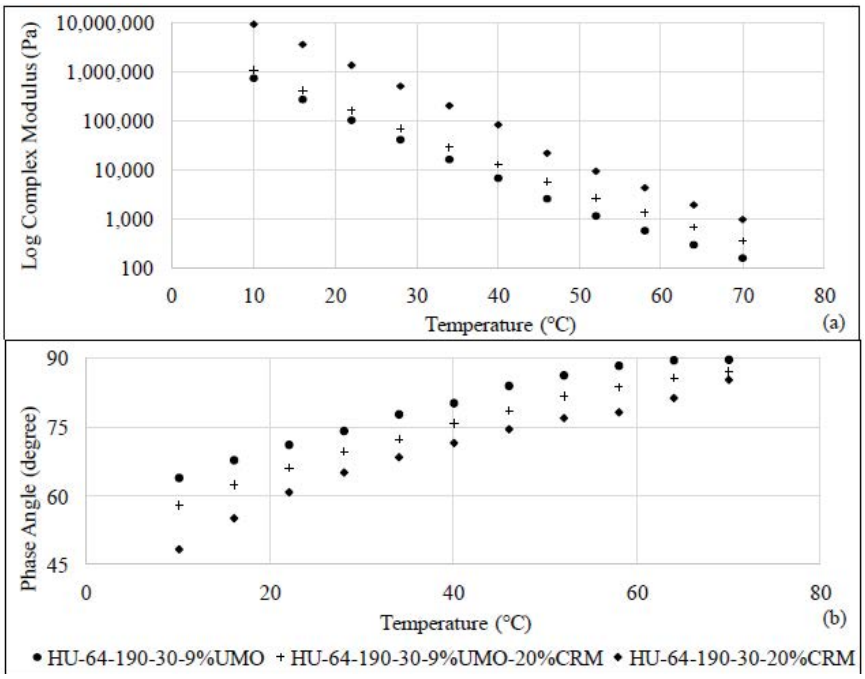

Figure 8: Temperature Sweep Viscoelastic Properties of Liquid Phase samples interacted with 9% UMO, 20% CRM or both at 190°C and 30Hz: (a) G* and (b) δ.

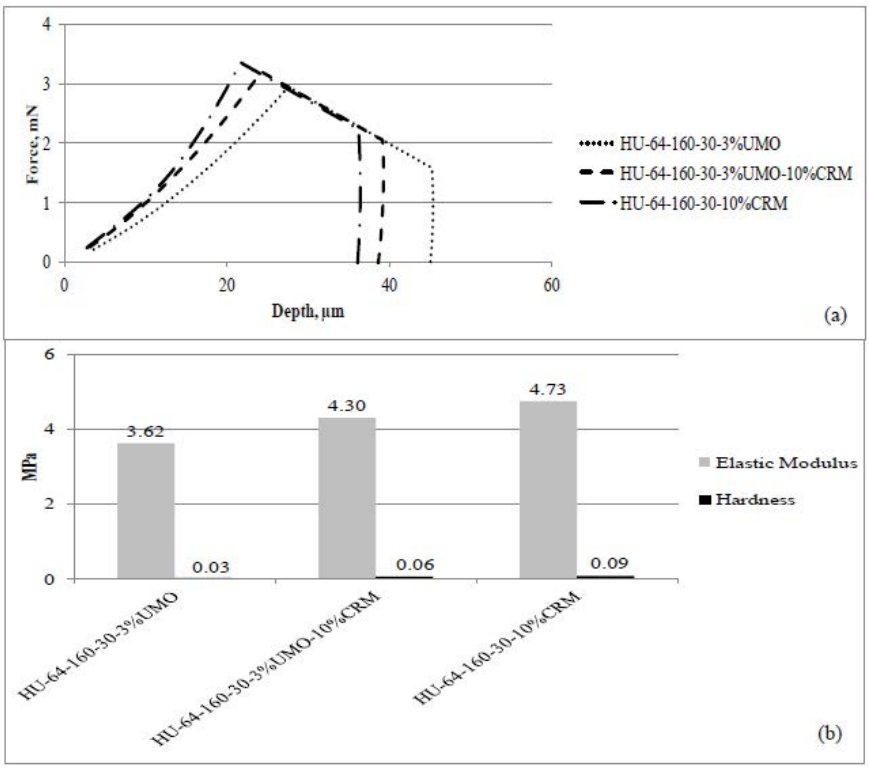

Figure 9: Micromechanical behavior of samples interacted at 160°C and 30Hz with 3% UMO, 10% CRM or both at 120 minutes interaction time: a) Force vs indentation depth profile, (b) Comparison of hardness and elastic modulus.

depth was recorded.

Figure 9b shows the hardness and elastic modulus values for the same samples. As shown in Figure 9b, a continuous increase in both the hardness and elastic modulus can be seen with the utilization of CRM with oil in asphalt and with CRMA only. The elastic modulus of samples was 3.62, 4.3, and 4.73 Mpa, for the asphalt samples modified with 3% UMO, 3% UMO with 10% CRM, and 10% CRM, respectively. On the other hand, the hardness of the samples was 0.03, 0.06, and 0.09 MPa. This indicates that at such a combination of interaction temperature (160°C) and interaction speed (30 Hz) the increase in the elastic modulus values occurs gradually with addition of CRM, whereas for the hardness, a major increase occurs when CRM is added to asphalt with UMO (almost double the values). This could be as a result of the higher absorption of the low molecular weight aromatics of asphalt by the CRM that lead to stiffer binder [14].

Figure 10 illustrates (a) the force vs. indentation depth profiles and (b) comparison of hardness and elastic modulus for the samples interacted at 160°C with 9% UMO, 20% CRM, or both modifiers after 120 minutes of interaction time.

Figure 10a shows a different trend than the samples interacted at 160°C with 30Hz with 3% UMO and 10% CRM. For the samples with 9% UMO only, the indentation depth is about 55 µm. However, upon addition of 20% CRM, a steep decrease in the indentation depth ranging around 45 µm is observed. On the other hand, for the samples with 20% CRM, the indentation depth was almost 23 µm. As illustrated in Figure 10b, an increase in both the hardness and elastic modulus values is evident after the addition of CRM. The elastic modulus was 2.9 MPa for the sample with 9% UMO and increased to 3.74, and 8.01MPa, for the samples modified by 9% UMO with 20% CRM, and 20% CRM, respectively. The same trend was seen for the hardness values that were 0.009, 0.04, and 0.36 MPa, for the aforementioned samples.

Figure 11 illustrates (a) the force vs. indentation depth profiles and (b) comparison of hardness and elastic modulus for the samples interacted at 190°C with 3% UMO, 10% CRM, or both modifiers after 120 minutes of interaction time.

Figure 11a shows a similar trend to the samples interacted at 160°C with 30 Hz with 3% UMO and 10% CRM. For the samples with 3% UMO only, the indentation depth is about 40 µm. However, upon addition of 10% CRM, we observe a minor decrease in the indentation depth to be about 35 µm. On the other hand, for the samples with 10% CRM, the indentation depth was almost 30 µm. As illustrated in Figure 11b, an increase in both the hardness and elastic modulus values is evident after the addition of CRM. The elastic modulus was 4.08 MPa for the sample with 3% UMO and increased to 4.85, and 5.34 MPa, for the samples modified by 3% UMO with 10% CRM, and 10% CRM, respectively. The same trend was seen for the hardness values that were 0.05, 0.09, and 0.12 MPa, for the aforementioned samples. It should be noticed that, upon increasing the interaction temperature from 160°C to 190°C, and with the utilization of 10% CRM with 3% UMO, the values of the hardness and elastic modulus show enhancement for the same sample conditions. This is direct result of the development in the asphalts internal structure that was proven in the temperature sweep section.

Figure 12 illustrates (a) the force vs. indentation depth profiles and (b) comparison of hardness and elastic modulus for the samples interacted at 190°C with 9% UMO, 20% CRM, or both modifiers after

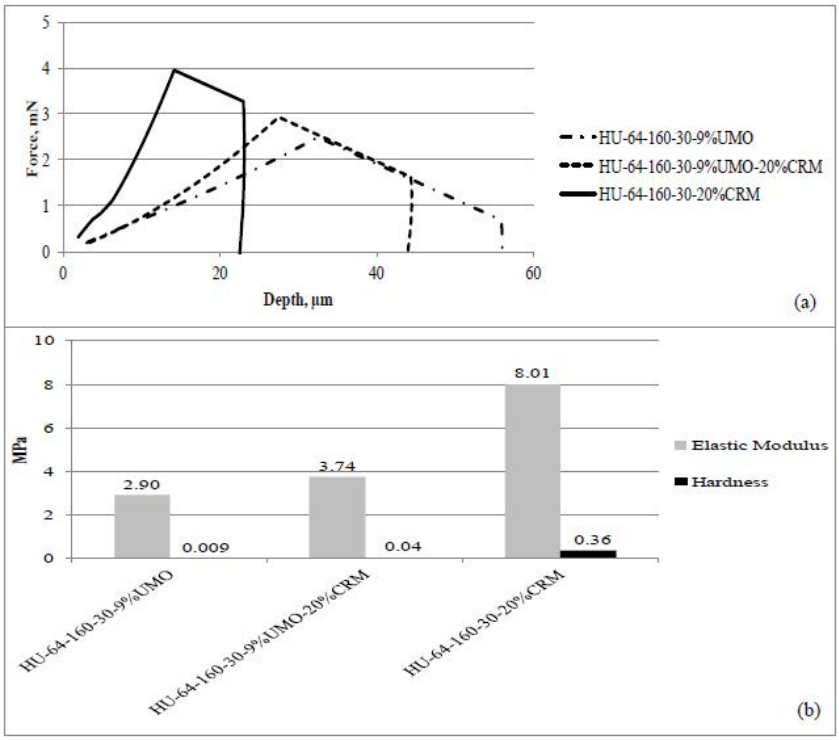

Figure 10: Micromechanical behavior of samples interacted at 160°C and 30Hz with 9% UMO, 20% CRM or both at 120 minutes interaction time: a) Force vs indentation depth profile, (b) Comparison of hardness and elastic modulus.

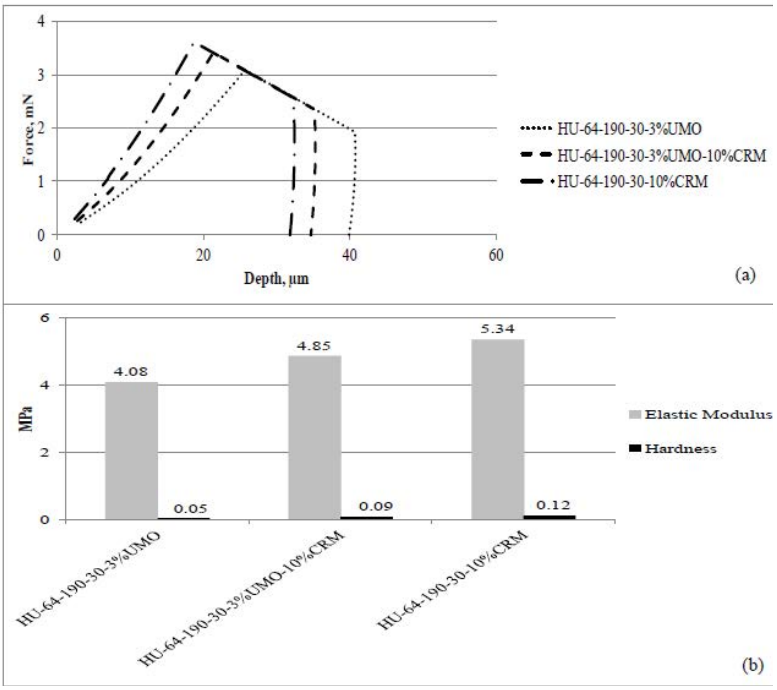

Figure 11: Micromechanical behavior of samples interacted at 190°C and 30Hz with 3% UMO, 10% CRM or both at 120 minutes interaction time: a) Force vs indentation depth profile, (b) Comparison of hardness and elastic modulus.

120 minutes of interaction time.

Figure 12a shows a different trend from that seen in the samples interacted at 190°C with 30 Hz with 3% UMO and 10% CRM. For the samples with 9% UMO only, the indentation depth is about 45 µm. However, upon addition of 20% CRM, we observe almost no change in the indentation depth ranging around 45 µm. On the other hand, for the samples with 20% CRM, the indentation depth was almost 20 µm. As illustrated in Figure 12b, a decrease in both the hardness and elastic modulus values is evident after the addition of CRM for the samples with UMO. The elastic modulus was 3.71 MPa for the sample with 9% UMO and decreased to 3.6, for the samples modified by 9% UMO with 20% CRM. However, a major increase in the elastic modulus (9.18 MPa) was recorded for the samples with 20% CRM only. The same trend was seen for the hardness values that were 0.004, 0.03, and 0.48 MPa, for the aforementioned samples.

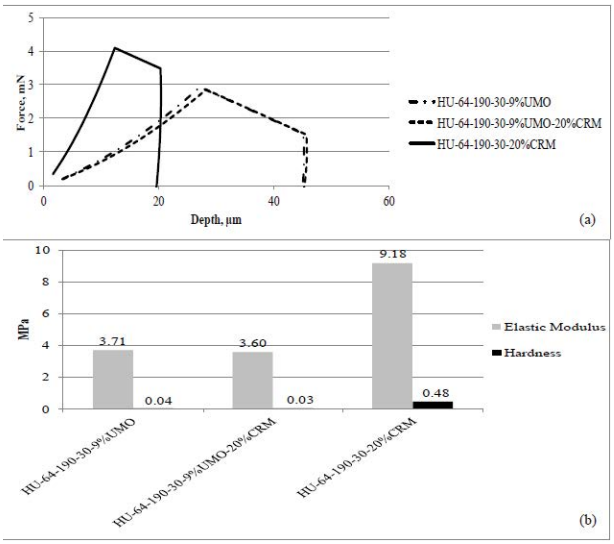

Figure 12: Micromechanical behavior of samples interacted at 190°C and 30Hz with 9% UMO, 20% CRM or both at 120 minutes interaction time: a) Force vs indentation depth profile, (b) Comparison of hardness and elastic modulus.

Conclusions

This work investigated the effect of the addition of UMO to neat and CRMA at different interaction conditions. The changes in the macro and micromechanical properties of the modified asphalts were investigated. It was found that the utilization of UMO only as a modifier to asphalt severely deteriorates the macro and micro mechanical properties of the binder because the UMO disrupts the asphalt intermolecular associations and internal network structure, in the absence of CRM. Combining CRM with UMO as modifiers to asphalt had better results for the lower percentages of modifiers (10% CRM with 3% UMO) over the higher percentage (20% CRM with 9% UMO). A better balance between the light molecular fractions absorbed by CRM from asphalt and the compensated amounts from UMO was achieved with the utilization of 3% UMO and 10% CRM. When employing a combination of 10% CRM and 3% UMO as modifiers to the binder, the utilization of the low interaction temperature (160°C) for the synthesis of modified asphalt was not sufficient to efficiently

develop the internal network structure of the modified asphalt that leads to enhancements in both the macro and micromechanical properties of the modified asphalt. Based on the current research work, it is suggested that when UMO is to be used in asphalt modification, it should be at a rate of less than 3%, and it should be combined with at least 10% CRM. The proposed synthesis conditions are an interaction temperature of 190°C and interaction speed of 30 Hz for a period of 120 minutes.

Acknowledgment

This material is based on the work supported by the National Science Foundation under Grant No. 0846861. Any opinions, findings, and conclusions or recommendations expressed in this material are those of the writer(s) and do not necessarily reflect the views of the National Science Foundation.

The writers would like to express their gratitude to Husky Energy for providing the asphalt used in this research work and also to Crumb Rubber Manufacturers for providing the crumb rubber used in this research work.

References

1. Agency EP. Wastes - Resource Conservation - Common Wastes & Materials. Available from: http://www.epa.gov/osw/conserve/materials/usedoil/oil.htm.
2. Wekumbura C, Stastna J, Zanzotto L (2007) Destruction and recovery of internal structure in polymer-modified asphalts. Journal of Materials in Civil Engineering 19: 227-232.
3. Stroup-Gardiner M (1995) Polymer Literature Review.
4. DeDene CD, You ZP (2014) The Performance of Aged Asphalt Materials Rejuvenated with Waste Engine Oil. International Journal of Pavement Research and Technology 7: 145-152.
5. Villanueva A, Ho S, Zanzotto L (2008) Asphalt modification with used lubricating oil. Canadian Journal of Civil Engineering 35: 148-157.
6. Ragab M, Abdelrahman M, Ghavibazoo A (2013) Performance Enhancement of Crumb Rubber-Modified Asphalts Through Control of the Developed Internal Network Structure. Transportation Research Record: Journal of the Transportation Research Board 2371: 96-104.
7. Bergerson D, Abdelrahman M, Ragab M (2014) Environmental Study of the Release of BTEX from Asphalt Modified with Used Motor Oil and Crumb Rubber Modifier. Int J Waste Resour 4: 165.
8. Tarefder RA, Zaman AM, Uddin W (2010) Determining hardness and elastic modulus of asphalt by nanoindentation. International Journal of Geomechanics 10: 106-116.
9. Tarefder RA, Faisal H (2012) Effects of dwell time and loading rate on the nanoindentation behavior of asphaltic materials. Journal of Nanomechanics and Micromechanics 3: 17-23.
10. Oyen ML, Ko CC (2007) Examination of local variations in viscous, elastic, and plastic indentation responses in healing bone. J Mater Sci Mater Med 18: 623-628.
11. Oliver WC, Pharr GM (1992) An improved technique for determining hardness and elastic modulus using load and displacement sensing indentation experiments. Journal of Materials Research 7: 1564-1583.
12. Stilwell N, Tabor D (1961) Elastic recovery of conical indentations. Proceedings of the Physical Society 78: 169.
13. Doerner MF, Nix WD (1986) A method for interpreting the data from depth-sensing indentation instruments. Journal of Materials Research. 1: 601-609.
14. Gawel I, Stepkowski R, Czechowski F (2006) Molecular interactions between rubber and asphalt. Industrial & Engineering Chemistry Research 45: 3044-3049.
15. Putman BJ, Amirkhanian SN (2006) Crumb rubber modification of binders: interaction and particle effects. Asphalt rubber 2006 conference, Palm Springs, USA.
16. Zanzotto L, Kennepohl GJ (1996) Development of rubber and asphalt binders by depolymerization and devulcanization of scrap tires in asphalt. Transportation Research Record: Journal of the Transportation Research Board 1530: 51-58.
17. Lu X, Isacsson U (2000) Modification of road bitumens with thermoplastic polymers. Polymer Testing 20:77-86.
18. Airey GD (2003) Rheological properties of styrene butadiene styrene polymer modified road bitumens. Fuel 82: 1709-1719